SYNOPSIS

Ph.D in Chemistry

Synthesis, Computational Assessment and Biological Evaluation of 2-amino-1,3,4-thiadiazoles and their Azo Derivatives

Submitted by

S. Kiruthika

19PHCHF002

Supervisor

Dr. V. Sharulatha

Assistant Professor (SG)

Department of Chemistry

Submitted to

Avinashilingam Institute for Home Science and Higher Education for Women, Coimbatore-641 043

April 2024

1. INTRODUCTION

Thiadiazoles are unique nucleus in pharma industry due to their documented more potent antimicrobial activity. The 1,3,4-thiadiazoles are well-known pharmacologically active compound. Thiadiazoles are the five-membered di unsaturated ring containing two carbon atoms, two nitrogen, and one sulfur atom. It is a planar aromatic and neutral ring system. The 1,3,4-thiadiazole moiety, it is characterized by a great *in vivo* stability making its derivatives biocompatible lacking toxicity. Mesoionic systems are dense, highly polarizable, and have a net neutral electron charge, allowing them to traverse cellular membranes and interact with biological targets with varying affinities. The presence of C=N molecular conjugation expands the biological activities **(Yijing *et al.*, 2012)**.

The 1,3,4-thiadiazole analogues containing azo dyes are very interesting group for new pharmaceuticals with a number of desirable effects including neuroprotective, antifungal, antibacterial, anti-inflammatory, antioxidants, and anti-cancer activity **(Budziak *et al.*, 2019, Karki *et al.*, 2011, Noolvi *et al.*, 2011, Almajan *et al.*, 2010 and Lamani *et al.*, 2009).** Hence, the privileged scaffold 1,3,4-thiadiazoles was chosen for synthesis and explore their antibacterial and antibiofilm activity.

- In the present work, **PHASE I** covers the synthesis and characterization of 2-amino-1,3,4-thiadiazoles and their azo derivatives.
- Firstly, 2-amino-1,3,4-thiadiazoles were prepared from eight different carboxylic acids and thiosemicarbazide in the presence of three different catalysts, and the compounds were characterized.
- Secondly, azo derivatives of 1,3,4-thiadiazoles were prepared by the diazotization method, and the compounds were characterized.
- **PHASE II** covers the density functional theory (DFT) studies such as Frontier molecular orbitals (FMO) analysis, Molecular electrostatic potential (MEP) map, geometry optimization, theoretical energy calculations, and Mulliken charge analysis of synthesized derivatives.
- **PHASE III** covers *in silico* molecular docking and ADMET analysis for the synthesized compounds.
- **PHASE IV** covers *in vitro* biological activities, including preliminary antibacterial, minimal inhibitory concentration (MIC), antibiofilm activity, and structure-activity relationship of synthesized compounds

1.1 OBJECTIVES

- ✓ To synthesize 2-amino-1,3,4-thiadiazole scaffolds and their azo derivatives.
- ✓ To characterize the compounds by UV-visible spectroscopy, FTIR spectroscopy, NMR spectroscopy, mass spectroscopy, and elemental analysis.
- ✓ To study the electronic and molecular properties of all synthesized derivatives using the computational DFT method.
- ✓ To find potent anti-microbial and anti-biofilm active compounds against *P. aeruginosa* and *S. aureus* organisms.
- ✓ To correlate *in vitro* and *in silico* studies by molecular docking analysis.
- ✓ To study the structure-activity relationship (SAR) of the synthesized compounds.

2. MATERIALS AND METHODS

2.1 Synthesis of 2-amino-1,3,4-thiadiazole derivatives (4a-h)

The 2-amino-1,3,4-thiadiazoles (**4a-h**) synthesized from reported procedure (**Santhosh *et al.*, 2015, Mahendrasinh *et al.*, 2013**). An equimolar mixture of substituted-2-oxo-1,2-dihydroquinolin-3-yl acetic acid/other acids (**1a-h**) and thiosemicarbazide in presence of conc. H_2SO_4 by reflux in a water bath at 100^0C as outlined in **Scheme I**. The obtained products were low yield. Hence, two different catalysts, *p*-toluene sulphuric acid and silica-supported sulphuric acid, were used to increase the yield and reduce the reaction time. The desired product was obtained in 1-6 hours and purified by recrystallization with a suitable solvent.

Synthesis of Azo-1,3,4-thiadiazole Derivatives (**Series I - 7a-d, 7g and 7h and Series II- 9a-d, 9g and 9h**)

The classic method used to synthesize azo compounds (**Series I - 7a-d, 7g, and 7h and Series II- 9a-d, 9g and 9h**), this method entails two steps of diazotization and coupling reactions represented in **Scheme II.** 0.02 g of substituted 2-amino-1,3,4-thiadiazoles was dissolved in 2 ml of dimethylformamide (DMF) and 0.6 ml of concentrated sulphuric acid (solution **A**). Solution **A** was stirred constantly for 20 minutes under ice-cold condition. 0.68g of dry sodium nitrite was slowly added to 1.2 ml of concentrated sulphuric acid over a period of 5 minutes with constant stirring under ice-cold condition. After completion of the addition, the stirring was continued for 10 minutes with heating at 65^oC (solution **B**). Diazotization

was carried out by dropwise addition of solution B to a well-stirred solution A under ice-cold conditions (solution **C**). Then, add a pinch of urea to solution **C**. Further, solution **C** was stirred for 1.5 hours under ice at a cold temperature below 10^{o}C.

0.076g of Resorcinol/β-naphthol (Coupling component) was dissolved in the mixture of NaOH (0.1g) and water (2 ml), then cooled to -10^{o}C (solution **D**). The above-resulting diazonium solution **C** was added dropwise to this well-stirred solution **D**, maintaining the temperature below 10^{o}C. The pH of the reaction mixture was maintained by adding a pinch of sodium carbonate. Then, the mixture was stirred for 1.5 hours under ice-cold conditions below 10^{o}C. The progress of the reaction was followed by TLC using an ethanol-hexane mixture (1:2). The resulting solid precipitate was filtered, washed with cold water, and dried **(Izzet Sener *et al.*, 2006)**. The crude product was purified by column chromatography**.**

SHIMADZU 1601 UV-visible spectrometer was used to record the UV-visible spectrum in DMSO solvent. The FTIR spectrum was recorded on the SHIMADZU instrument to investigate the functional groups (400-4000 cm^{-1}). The nuclear magnetic resonance (^{1}H NMR and ^{13}C NMR) spectrum was recorded on a Bruker 400 MHz instrument in a DMSO-d_6 solvent. Mass spectra were analysed using the Jeol GC-mate –II instrument. Thermo Fisher Scientific – Flash smart V CHNS instrument was used to record the elemental composition.

Gaussian 16 w software and Gauss view were used for computational DFT analysis. The basis set of the DFT calculation is to be B3LYP/6-31G' + (d p). The docking study was performed using the Autodock Vina Software (**Oleg *et al.*, 2010**) against two proteins, namely LasR (PDB ID: 3IX4) of *Pseudomonas aeruginosa* and AgrA (PDB ID: 4G4K) of *Staphylococcus aureus*. ADMET analysis was performed by Swiss ADME and pkcsm ADMET online web tools**.**

Kirby- Bauer method was used for antibacterial activity against *Staphylococcus aureus* MTCC 3160 and *Pseudomonas aeruginosa* MTCC 2350 cultures**. Wiegand *et al.*, 2008** reported a method used to find the MIC of synthesized compounds. The biofilm assay was carried out using the **Sharmaradi *et al.*, 2019** reported method. Biofilm morphology was performed as previously reported methods on glass coverslips for *Pseudomonas aeruginosa* (**Patil *et al.*, 2017; Kalia *et al.*, 2015 and Valliammai *et al.*,**

Research Plan of the Present Work

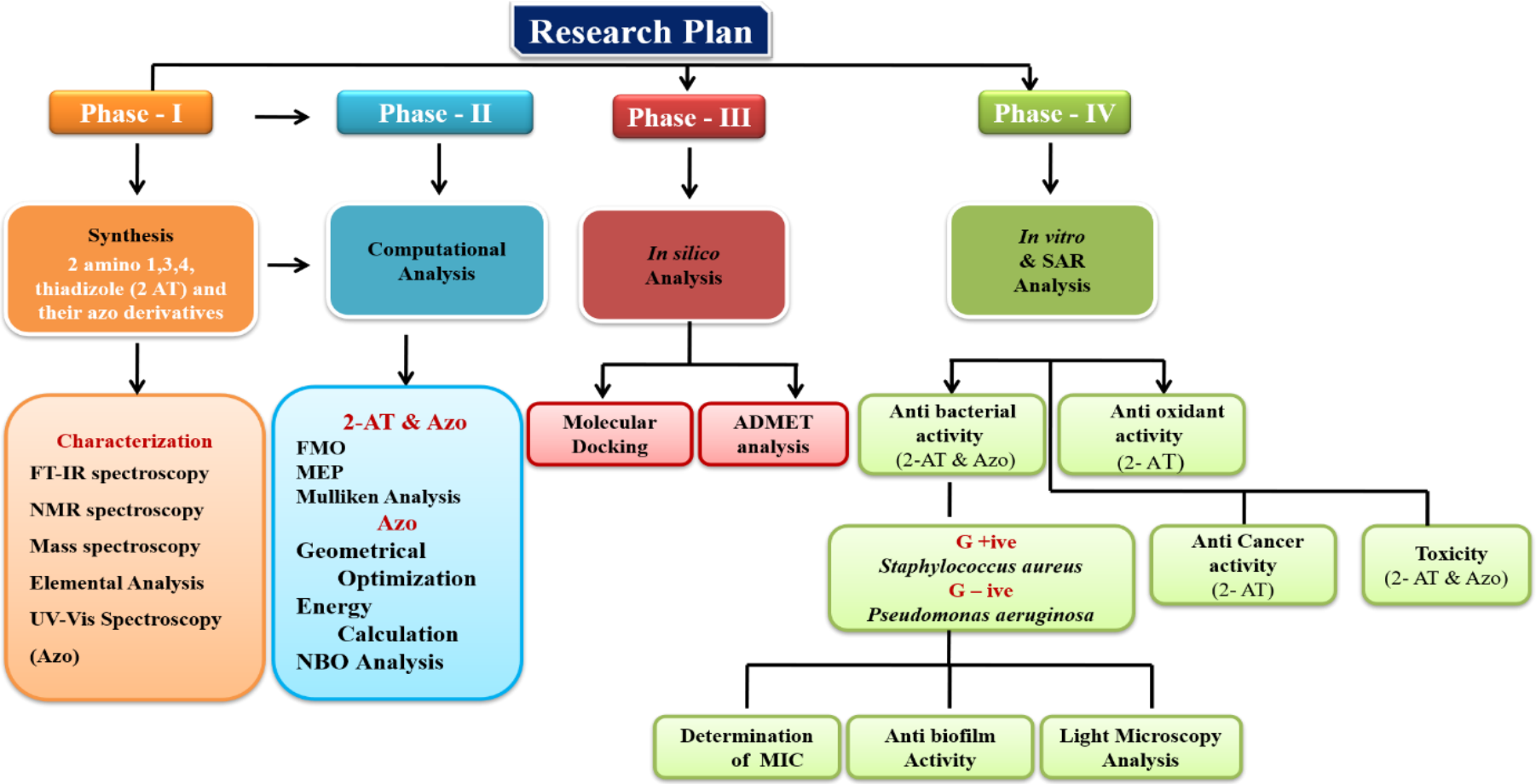

Flow Chart 1 Research plan of the present work

and *Staphylococcus aureus* through light microscopy analysis (40x magnification). The MTT assay was performed to determine the cytotoxicity against MOLT-3 leukemia cancer cells and peripheral blood lymphocyte cells (**Igarashi & Miyazawa, 2011**). DPPH assay was performed for the antioxidant activity (**Hatano *et al.*, 1988**).

3. RESULTS AND DISCUSSION

3.1 PHASE I Synthesis and Characterization

3.1.1 Synthesis of 2-amino-1,3,4-thiadiazole Derivatives

Synthesized compounds were stable at room temperature and white to yellow colour solids were obtained with 53-81% yields (**Table 1)**. The recyclable silica-supported sulphuric acid catalyst was successfully employed for three runs without loss in their activity.

Scheme I Synthesis of 2-amino-1,3,4-thiadiazole Derivatives

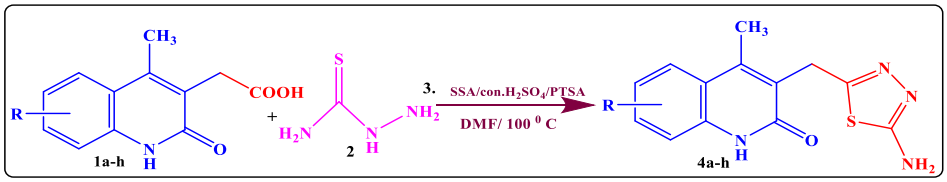

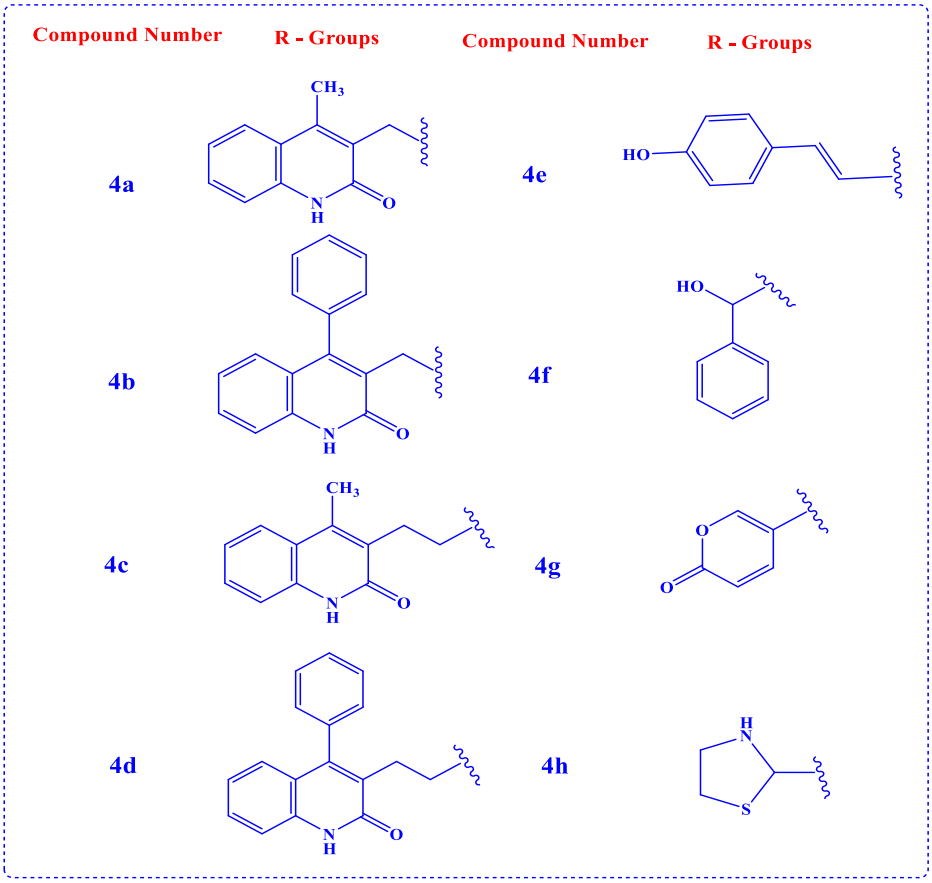

Table 1: Performance of three different catalyst in the synthesis of 2-amino-1,3,4-thiadiazole derivatives

Compounds	Reaction Temperature (^{0}C)	Melting Point (^{0}C)	Conc.H_2SO_4 Catalyst		p-Toluene sulphonic acid catalyst		Silica supported sulphuric acid catalyst	
			Reaction Time (h)	Yield (%)	Reaction Time (h)	Yield (%)	Reaction Time (h)	Yield (%)
4a	100	241	3	63	2	51	1	81
4b	100	229	4	56	2	50	1	74
4c	100	231	3.5	58	1.5	31	3	72
4d	100	227	5	71	2	50	4	71
4e	100	170	16	68	1	63	1	68
4f	100	82	23	41	4	39	5	61
4g	100	123	1.5	80	1.5	25	1.5	86
4h	100	230	2	53	8	Trace amount	0.5	53

3.1.2 Spectral Characterization

The UV-visible, FTIR, ^{1}H NMR and ^{13}C NMR, mass spectroscopy and CHNS analysis used to predict the structure of the synthesized compounds.

3.1.2.1 FTIR Spectroscopy Analysis of 3-((5-amino-1,3,4-thiadiazol-2-yl)methyl)-4-methylquinolin-2(1*H*)-one (4a)

The characteristic absorption band at 3443 cm^{-1} assigned to N-H stretching, and the N-H bending peak was absorbed at 1433 cm^{-1}. The strong band at 1637 cm^{-1} denoted the presence of C=N, and a sharp peak at 762 cm^{-1} corresponds to the C-S-C stretching belonging to the thiadiazole ring. The characteristic frequency 1103 cm^{-1} observed as a medium intense peak indicates the existence of the N-N group of the thiadiazole ring. The peak observed at 1397 cm^{-1} was due to the presence of C-N bending vibration. The carbonyl stretching frequency corresponding to C=O of the quinoline ring was observed at 1792 cm^{-1}. The FTIR spectrum of compound **4a** is shown in **Figure 1.**

3.1.2.2 ^{1}H NMR Spectroscopy Analysis of 3-((5-amino-1,3,4-thiadiazol-2-yl)methyl)-4-methylquinolin-2(1*H*)-one (4a)

The ^{1}H NMR spectra of compound **4a** displayed eight sets of signals shown in **Figure 2 and Table 2**. The proton of the NH group resonates at most downfield around δ_H 11.01 ppm as a broad singlet. The two aryl protons belonging to the C_1-H and C_2-H of quinoline rings were observed as two triplets δ_H 7.22 – 7.19 ppm and δ_H 7.50 – 7.46 ppm. The peaks around δ_H 7.33 – 7.30 ppm and δ_H 7.78 – 7.76 ppm attributed to C_3-H and C_6-H aromatic protons observed as two doublets. A tiny broad singlet peak observed at δ_H 3.33 ppm

attributed to NH_2 of thiadiazole ring. Both the NH and NH_2 proton signals appeared as broad singlets due to quadrupolar interactions of the nitrogen (^{14}N) nucleus. Quadrupolar interactions in the solution state of the nucleus (^{14}N) effectively contribute to NMR relaxation, resulting in broad unresolved signals **(Bartova *et al.*, 2020)**. A singlet at δ_H 3.67 ppm is assigned to the CH_3 protons. Furthermore, the singlet observed at about δ_H 2.39 ppm denoted the presence of CH_2 protons.

3.1.2.3 ^{13}C NMR Spectroscopy Analysis of 3-((5-amino-1,3,4-thiadiazol-2-yl)methyl)-4-methylquinolin-2(1*H*)-one (4a)

The ^{13}C NMR spectrum of compound **4a** showed carbonyl carbon at δ_C 172.54 ppm. The seven aromatic carbons of the quinoline ring appeared in the range of δ_C 115.61 (C_1, C_2), δ_C 120.87(C_9), δ_C 122.21(C_3, C_6), δ_C 125.52 (C_5), δ_C 130.64 (C_4) and δ_C 137.84 (C_{10}) ppm. The two thiadiazole carbon signals at δ_C 161.91 (N=C_{12}-S-N) ppm and δ_C 144.63 (N=C_{14}-N-C) ppm indicated the formation of thiadiazole ring in compound **4a**. The signals observed at δ_C 15.65 (C_{19}) ppm and δ_C 32.71 (C_{11}) due to the presence of methyl and methylene carbons, respectively (**Figure 3**).

3.1.2.4 Mass Spectrum of 2-amino- 1,3,4-thiadiazole derivatives

The calculated molecular ion peak for compound **4a** was found *m/z* = 272.07, and the observed *m/z* peak at 272.01 confirmed the proposed structure. Furthermore, the fragmented peaks were observed at *m/z* 135, 192, 208, and 226, respectively. The mass spectrum of compound **4a** is shown in **Figure 4**.

3.1.2.5 CHNS Analysis of 2-amino- 1,3,4-thiadiazole derivatives

The obtained elemental composition of carbon - 57.12%, hydrogen – 4.66 %, nitrogen – 20.46 %, and sulfur- 10.99 % was similar to the calculated elemental composition of carbon – 57.75 %, hydrogen – 4.66 %, nitrogen 20.72 %, and sulfur – 11.86 % confirms the proposed structure of compound **4a**.

Similarly, the other 2-amino-1,3,4-thiadiazole derivatives (**4b-4h**) were characterized.

Spectral Characterization of 3-((5-amino-1,3,4-thiadiazol-2-yl)methyl)-4-methylquinolin-2(1*H*)-one (4a)

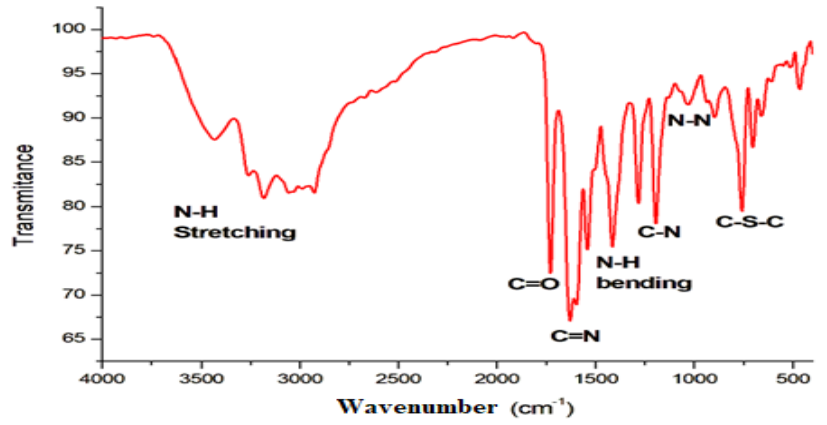

Figure 1 FTIR spectrum of 3-((5-amino-1,3,4-thiadiazol-2-yl)methyl)-4-methylquinolin-2(1*H*)-one (4a)

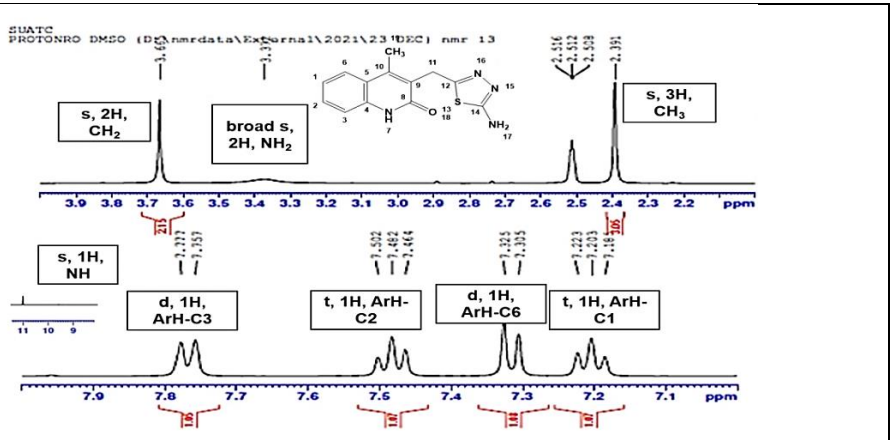

Figure 2 ^{1}H NMR spectrum of 3-((5-amino-1,3,4-thiadiazol-2-yl)methyl)-4-methylquinolin-2(1*H*)-one (4a)

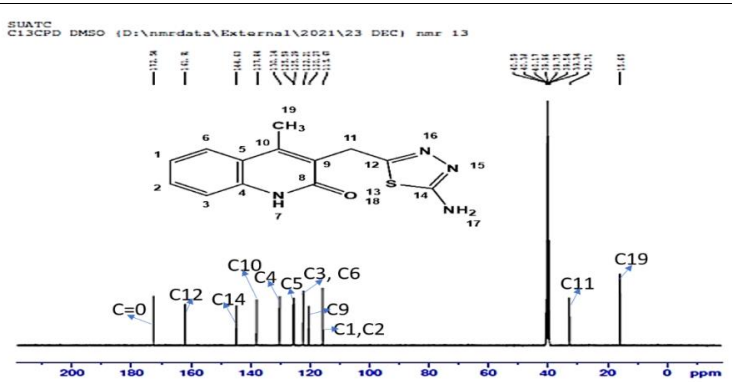

Figure 3 ^{13}C NMR spectrum of 3-((5-amino-1,3,4-thiadiazol-2-yl)methyl)-4-methylquinolin-2(1*H*)-one (4a)

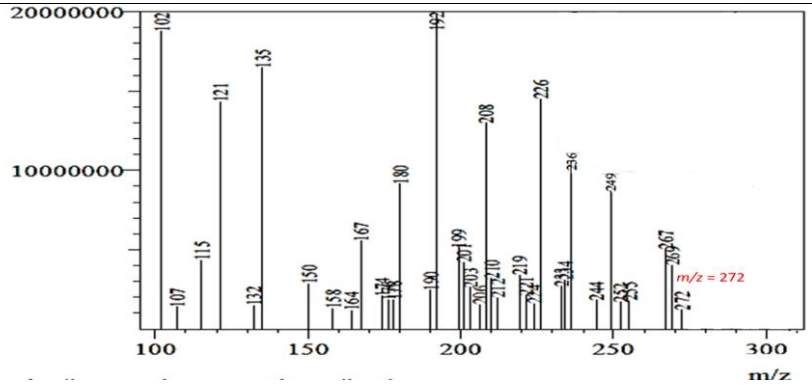

Figure 4 Mass spectrum of 3-((5-amino-1,3,4-thiadiazol-2-yl)methyl)-4-methylquinolin-2(1*H*)-one (4a)

Table 2 NMR Characterization of 3-((5-amino-1,3,4-thiadiazol-2-yl)methyl)-4-methylquinolin-2(1*H*)-one (4a)

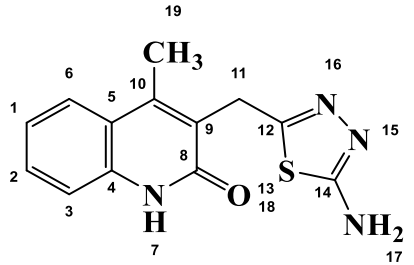

^{1}H NMR				^{13}C NMR	
^{1}H NMR -Chemical Shift (δ, ppm)/Multiplicity	**J Value (Hz)**	**No. of Protons**	**Assigned to**	**^{13}C NMR Chemical Shift (δ, ppm)**	**Assigned to**
11.01/s	-	1H	N-H	15.7	C_{19}
7.78-7.76/d	8.0	1H	C_3-H	32.7	C_{11}
7.50-7.46/t	15.0	1H	C_2-H	115.6	C_1, C_2
7.33-7.30/d	8.0	1H	C_6-H	120.9	C_9
7.22-7.19/t	15.0	1H	C_1-H	122.2	C_3, C_6
3.67/s	-	2H	CH_2	125.5	C_5
3.33/s	-	2H	NH_2	130.6	C_4
2.39/s	-	3H	CH_3	137.8	C_{10}
-	-	-	-	144.6	C_{14}
-	-	-	-	161.9	C_{12}
-	-	-	-	172.5	C_8

3.1.2 Synthesis of Azo-1,3,4-thiadiazole Derivatives

Synthesis of azo-1,3,4-thiadiazole derivatives was presented in **Scheme II**. The obtained azo compounds were of various color ranges from yellow to brown with 72-97 % yields presented in **Table 2**.

Scheme II Synthesis of Azo-1,3,4-thiadiazole Derivatives

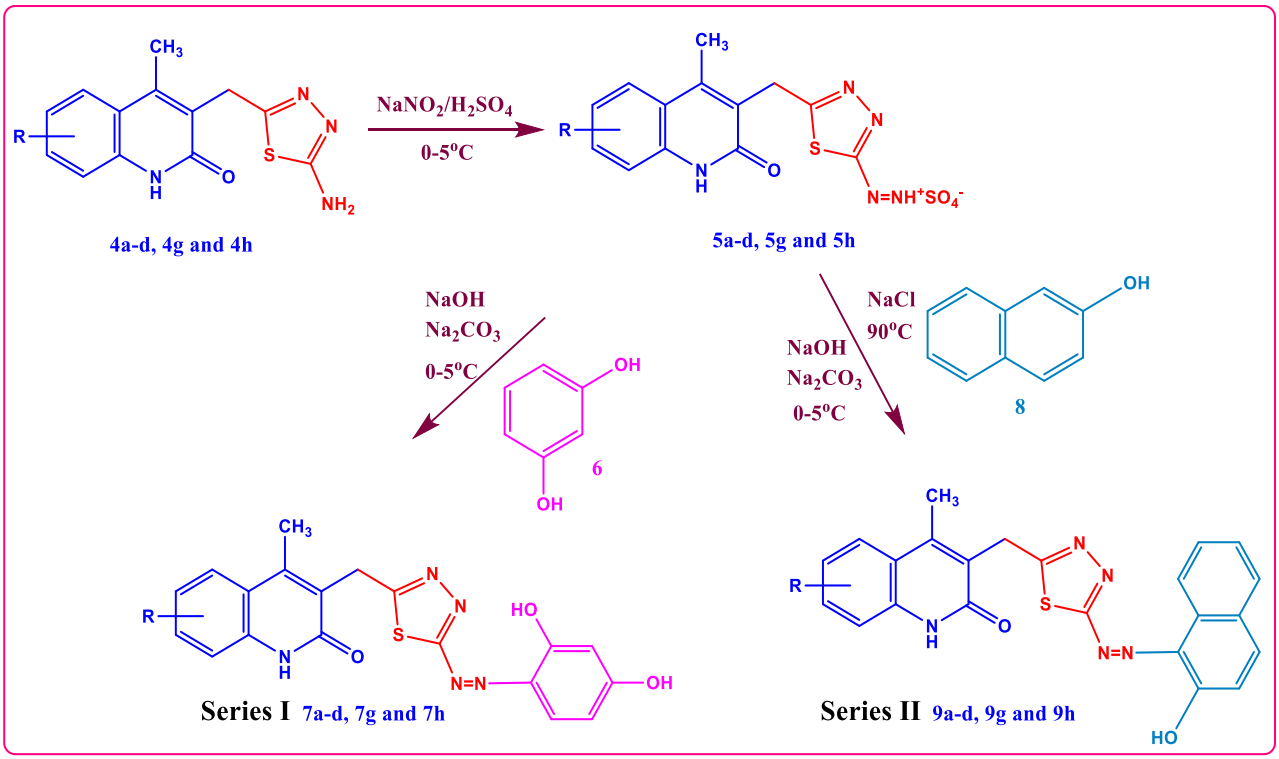

Table 3 Physical Data of Synthesized Azo-1,3,4-thiadiazole Derivatives

Compound	Colour	Yield (%)	Melting Point (^{0}C)
7a	Yellow	93	168
7b	Yellow	85	172
7c	Light brown	97	120
7d	Light brown	79	122
7g	Orange	72	156
7h	Yellowish orange	96	186
9a	Brown	76	170
9b	Greenish yellow	86	162
9c	Dark brown	74	150
9d	Brown	81	140
9g	Brown	80	98
9h	Dark brown	71	106

3.1.3 Spectral Characterization Azo-1,3,4-thiadiazole Derivatives

3.1.3.1 UV-Visible Spectrum of 3-((5-((2,5-dihydroxyphenyl)diazenyl)-1,3,4-thiadiazol-2-yl)methyl)-4-methyl quinolin-2(1*H*)-one (7a)

In UV-visible spectrum four sets of bands were observed in the DMSO solvent. The spectra showed two absorption bands at 256 and 316 nm was assigned for the π-π* transition, and the bands at 373 and 404 nm indicated the n-π* transitions**.** The observed highest molar extinction coefficients indicated that the synthesized compounds are *trans* isomers (**Wallace *et al.*, 1952)**.

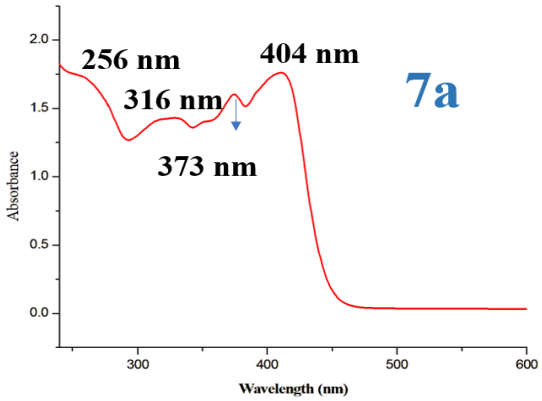

Figure 5 UV-Visible Spectrum of 3-((5-((2,5-dihydroxyphenyl)diazenyl)-1,3,4-thiadiazol-2-yl)methyl)-4-methyl quinolin-2(1H)-one (7a)

3.1.3.2 FTIR Spectrum of 3-((5-((2,5-dihydroxyphenyl)diazenyl)-1,3,4-thiadiazol-2-yl)methyl)-4-methyl quinolin-2(1*H*)-one (7a)

The FTIR spectra showed N-H stretching of the quinoline ring at 3200 cm^{-1}. The band observed at 3431 cm^{-1} was due to the O-H stretching vibration. The sharp peak at 1643 cm^{-1} denotes the -N=N- azo formation. Three sharp peaks at 1589 cm^{-1}, 1465 cm^{-1}, and 679 cm^{-1} indicated the presence of C=N, C-N, and C-S-C groups belonging to the thiadiazole ring. The C=O stretching was observed at 1056 cm^{-1}. The FTIR spectrum of compound **7a** is portrayed in **Figure 6**.

3.1.3.3 ^{1}H NMR Spectrum of 3-((5-((2,5-dihydroxyphenyl)diazenyl)-1,3,4-thiadiazol-2-yl)methyl)-4-methyl quinolin-2(1*H*)-one (7a)

Proton NMR signals of compound **7a** are displayed in **Figure 7 and Table 4**. The ^{1}H NMR spectra of **7a** displayed the resorcinol ring aromatic protons as two doublet and one singlet peaks at δ_H7.26-7.28 (C_{18}-H), δ_H 7.39-7.41 (C_{17}-H) and δ_H 8.85 (C_{20}-H) respectively. The quinoline ring protons C_1-H and C_2-H appeared as multiplet in the region of δ_H7.48 – 7.57 ppm, and the C_3-H and C_6-H protons were observed as two doublets at δ_H 8.11 -8.13 and δ_H 8.41 – 8.43 ppm respectively. The methyl protons were observed as singlet at δ_H 3.21, and the -CH_2- protons appeared as singlet in the region of δ_H 3.27 ppm. The N-H proton belonging to the quinoline ring was observed as a broad singlet at δ_H 11.99 ppm. The two OH protons of the resorcinol ring appeared as two singlets at δ_H 9.18 ppm and δ_H 8.89 ppm, respectively.

3.1.3.4 ^{13}C NMR of Spectrum of 3-((5-((2,5-dihydroxyphenyl)diazenyl)-1,3,4-thiadiazol-2-yl)methyl)-4-methyl quinolin-2(1*H*)-one (7a)

The aromatic carbon signals were observed in the range of δ_C 108.5 to δ_C 135.5 ppm. The signal at δ_C 148.0 and δ_C 156.0 ppm corresponds to the two C_{25}=N and C_{23}=N carbons belonging to the thiadiazole ring. The peak observed at δ_C 156.6 and δ_C 163.6 ppm due to the presence of two C-OH groups in the resorcinol ring. A signal at δ_C 166.9 attributed to the C=O carbon in the quinoline ring. The ^{13}C NMR spectrum is shown in **Figure 8.**

3.1.3.5 Mass Spectrum of 3-((5-((2,5-dihydroxyphenyl)diazenyl)-1,3,4-thiadiazol-2-yl)methyl)-4-methyl quinolin-2(1*H*)-one (7a)

The calculated molecular peak was m/z at 393.09, and the observed molecular ion peak at m/z = 394.45 was the M^++1 peak. The other fragment peaks observed at m/z 115, 271, 294, and 308 shown in **Figure 9**.

Similarly, the other azo-1,3,4-thiadiazole derivatives were characterized.

Spectral Characterization of 3-((5-((2,5-dihydroxyphenyl)diazenyl)-1,3,4-thiadiazol-2-yl)methyl)-4-methyl quinolin-2(1*H*)-one (7a)

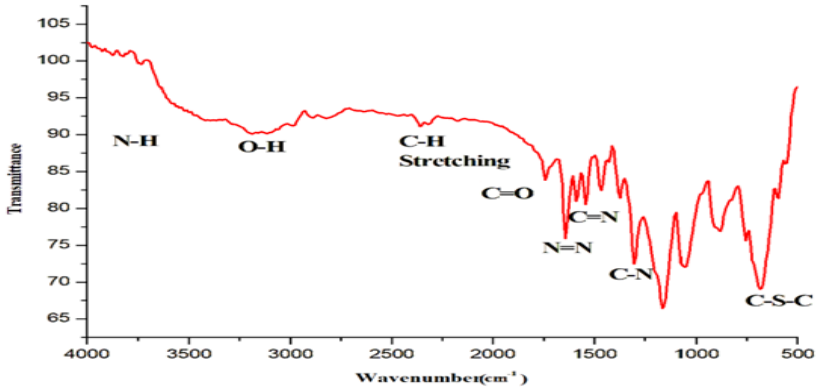

Figure 6 FTIR Spectrum of 3-((5-((2,5-dihydroxyphenyl)diazenyl)-1,3,4-thiadiazol-2-yl)methyl)-4-methylquinolin-2(1H)-one (7a)

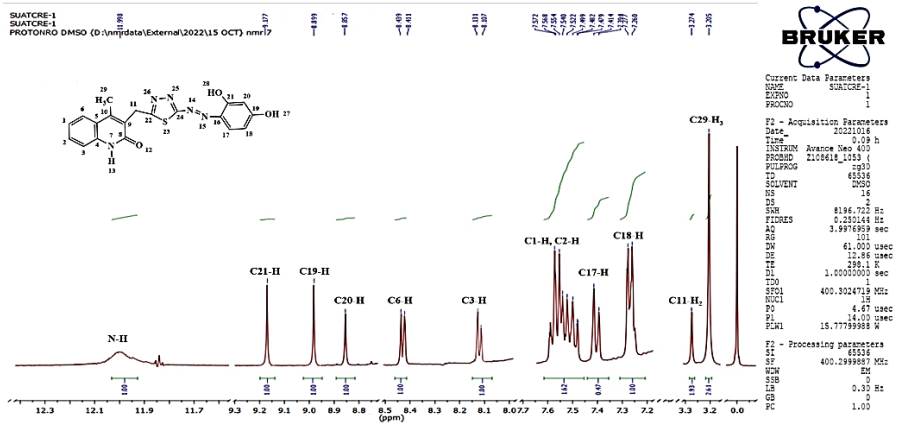

Figure 7 ^{1}H NMR Spectrum of 3-((5-((2,5-dihydroxyphenyl)diazenyl)-1,3,4-thiadiazol-2-yl)methyl)-4-methylquinolin-2(1H)-one (7a)

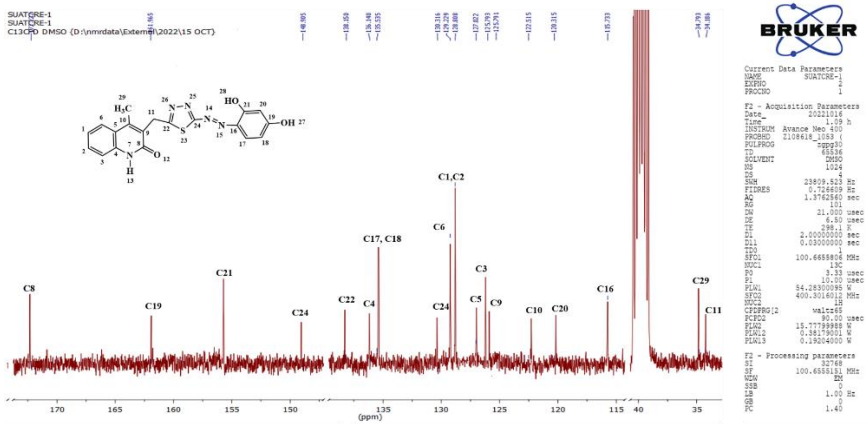

Figure 8 ^{13}C NMR Spectrum of 3-((5-((2,5-dihydroxyphenyl)diazenyl)-1,3,4-thiadiazol-2-yl)methyl)-4-methylquinolin-2(1H)-one (7b)

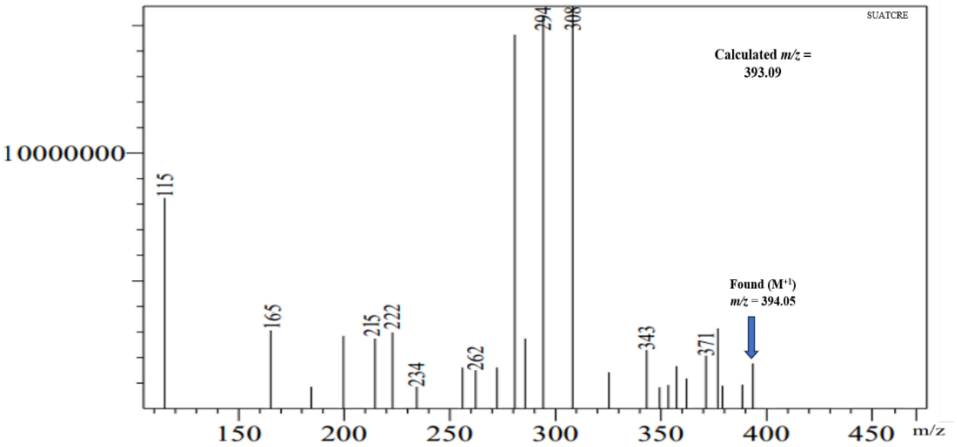

Figure 9 Mass Spectrum of (E)-3-((5-((2-hydroxynaphthalen-1-yl)diazenyl)-1,3,4-thiadiazol-2-yl)methyl)-4-methylquinolin-2(1H)-one (9a)

Table 4 Spectral Characterization of 3-((5-((2,5-dihydroxyphenyl)diazenyl)-1,3,4-thiadiazol-2-yl)methyl)-4-methylquinolin-2(1*H*)-one (7a)

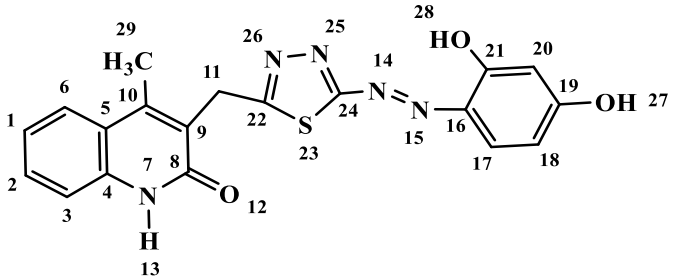

^{1}H NMR				^{13}C NMR			
^{1}H NMR -Chemical Shift (δ, ppm)/Multiplicity	**J Value (Hz)**	**No. of Protons**	**Assigned to**	**^{13}C NMR Chemical Shift (δ, ppm)**	**Assigned to**	**^{13}C NMR Chemical Shift**	**Assigned to**
3.21/s	-	3H	C_{11}-H_2	34.2	C_{12}	135.5	C_{30}
3.27/s	-	2H	C_{29}-H_3	34.8	C_{11}	136.1	C_4
7.26-7.28/d	8.0	1H	C_{18}-H	115.7	C_1	138.1	C_{22}
7.39-7.41/d	8.0	1H	C_{17}-H	120.3	C_6	148.9	C_{24}
7.48-7.57/m	-	2H	C_1-H, C_2-H	122.5	C_3	155.5	C_{21}
8.11-8.13/d	8.0	1H	C_3-H	125.7	C_5	161.9	C_{19}
8.41-8.44/d	8.0	1H	C_6-H	125.8	C_9	171.2	C_8
8.86/s	-	1H	C_{20}-H	127.0	C_{19}		
8.99/s	-	1H	C_{19}-OH	128.8	C_{20}		
9.18/s	-	1H	C_{21}-OH	129.2	C_{28}		
11.9/s	-	1H	N-H	130.3	C_{29}		

3.2 PHASE II - Computational Analysis

3.2.1 Frontier Molecular orbital (FMO) and Quantum Chemical Descriptors of 2-amino-1,3,4-thiadiazole Derivatives

The synthesized compounds showed HOMO energies between -9.3716 eV to -4.3886 eV and LUMO's between -3.3606 to -0.5469. The compound **4f** was predicted to have high-lying HOMO (-4.3886 eV), readily donating electrons. Furthermore, the compound **4g's** LUMO was found to be -3.4014 eV considered as best electron acceptor. Compound **4d** exhibited a higher-lying HOMO (-5.0161 eV), indicating the most potent electron donor. However, its lower energy gap (-3.4107 eV) suggested more excellent bioactivity. Compound **4d's** high HOMO and minimal GAP indicate its soft nature, making it more reactive than hard molecules by facilitating electron transfer to acceptors, thereby enhancing its biological activity (**Hager *et al.*, 2020; Ismael *et al.*, 2020**). The calculated higher dipole moment for compound **4d** is 6.5 Debye, with increased active electrons and enhanced biological activity (**Rahoumani *et al.*, 2019**).

3.2.2 Geometry Optimization, FMO and Quantum Chemical Descriptors of Azo-1,3,4-thiadiazole Derivatives

Geometry optimization revealed that the *trans*-isomers are more stable structures than the *cis*-isomers. Compound **9d** showed the lowest energy gap, -2.4544 eV, which is soft and more bioactive. Moreover, the higher the dipole moment of the compound **9d**, the more active the electron is and has higher biological activity (**Rahoumani *et al.*, 2019)**. Electrophilicity, a measure of energy stabilization phenomena related to the transfer of electrons from the environment to the molecular system, signifies the compound's reactivity and electrophilic behaviour.

3.3 PHASE III *In silico* Analysis

3.3.1 Molecular Docking Analysis

3.3.1.1 Docking Interactions of 2-amino-1,3,4-thiadiazoles

2-amino-1,3,4-thiadiazole derivatives (**4a-h**) showed different types of interaction with amino acid residues in two targets, LasR and AgrA. The 2-amino-1,3,4-thiadiazole derivatives displayed the binding affinity range -4.9 to -8.3 kcal/mol with AgrA protein and -

4.8 to -8.0 kcal/mol against LasR protein. Additionally, the compound **4d** showed the highest binding scores with both targets.

3.3.1.2 Docking Interaction of Azo-1,3,4-thiadiazole derivatives

The azo-1,3,4-thiadiazole derivatives involved different types of interactions such as π - π, π -alkyl, and hydrogen bonds with the target proteins. Azo compounds exhibit binding scores in the range between -5.1 to -10.1 kcal/mol against AgrA protein and -5.6 to -9.6 against LasR protein. Notably, 1,3,4-thiadiazole substituted with quinoline and naphthol rings showed the highest binding interaction score than the other compounds. Compound **9d** showed the highest binding scores, -10.1 with AgrA protein and -9.6 with the LasR target site, which is higher than the standard drug gentamycin, showed -8.2 with LasR and -6.4 with AgrA, respectively.

3.3.2 ADMET Analysis

3.3.2.1 ADMET Analysis of of 2-amino-1,3,4-thiadiazole Derivatives

Lipinski's "rule of five" speculates that a candidate molecule **4a-h** is likely to be orally active if it complies with the rule without any violations, including molecular weight (MW) < 500, a calculated octanal/water partition coefficient (log P) < 4.15, fewer than five hydrogen bond donors, fewer than ten hydrogen bond acceptors, and a topological polar surface area (TPSA) < 140 Å. Skin sensitivity indicated no sensitivity for compounds **4a-4h**.

3.3.2.2 ADMET Analysis of Azo-1,3,4-thiadiazole Derivatives

The compounds **7a-d, 7g, 7h, 9a,9c and 9g, 9h** obeyed Lipinski's rule of five and showed 0 violations, while the compounds **9b** showed one violation: M Log P >4.15 and **9d** showed two violations: MW>500, M Log P> 4.15. The azo derivatives of **7a-d, 7g, 7h and 9a-d, 9g, 9h** have –N=N- problematic functional group. The bioactive score of 0.55 for all compounds except the **9d** (0.17) indicated that all synthesized derivatives are biologically active. The synthesized molecules were found to have better drug-likeness and ADME properties.

3.4 PHASE IV- *In vitro* Analysis

3.4.1 Antibacterial Analysis of 2-amino-1,3,4-thiadiazole Derivatives

The compounds **4a-4h** exhibited moderate to high antibacterial activity against the tested pathogens. Notably, compounds **4a, 4b**, and **4d** displayed the most potent antibacterial activity against both *S. aureus* and *P. aeruginosa*, with inhibition zones comparable to the reference antibiotic gentamycin at a concentration of 100 µg/mL. The potent activity may be attributed to the nature of the quinoline ring.

3.4.2 Antibiofilm Analysis of 2-amino-1,3,4-thiadiazoles

Biofilm formation is a critical virulence factor of pathogenic microorganisms. The effect of compounds **4a-4h** on biofilm formation was assessed using Gram-positive *S. aureus* and Gram-negative *P. aeruginosa*. Compound **4d** significantly disrupted biofilm formation by 75 % at ½ MIC and 72 % at ¼ MIC against *S. aureus*, compared to the reference compound gentamycin, which inhibited biofilm formation by 88 % at ½ MIC and 81 % at ¼ MIC.

For *P. aeruginosa*, compound **4d** demonstrated high biofilm disruption, with 92 % inhibition at ½ MIC and 77 % at ¼ MIC respectively. Morphological analysis through light microscopy analysis confirmed the disruption of biofilm against both the tested organisms.

3.4.3 Antioxidant Analysis of 2-amino-1,3,4-thiadiazoles

Antioxidant activity was performed to test the scavenging ability of the quinoline-substituted thiadiazoles (**4a-d**), and a comparative study was carried out with their quinoline acids (**1a-d**). The DPPH radical reduces hydrazine when vital hydrogen donors for antioxidants are present, altering the reaction color from violet to yellow. Compound **1a** displays a strong inhibition of DPPH, as shown by the percentage inhibition value of 83 %, and it required 58.0 µg/ml to reduce the 50 % of DPPH. The standard ascorbic acid reduces DPPH at IC_{50} = 11.7 µg/mL. In contrast, the compounds **4a-d** showed a higher antioxidant activity than **1a-d**.

3.4.4 Anticancer Analysis of 2-amino-1,3,4-thiadiazoles

In order to evaluate the anticancer activity against MOLT-3 human leukemia cell lines and the etoposide were used as a positive control. Fused 2-amino 1,3,4-thiadiazoles with IC_{50} > 100µg/mL in MTT assay considered noncytotoxic.

3.4.5 Antibacterial Activity of Azo-1,3,4-thiadiazole Derivatives

The antibacterial activity results revealed that some compounds displayed varying effects on the growth of the *Staphylococcus aureus* and *Pseudomonas aeruginosa* strains. All the synthesized compounds exhibited potent to moderate activity against *Staphylococcus aureus* organism and moderate to poor activity against *Pseudomonas aeruginosa*. Compound **9d** showed potent activity against *Staphylococcus aureus* with a 24 mm zone of inhibition at 100µg/ mL, higher than standard gentamycin 14 mm zones.

3.4.6 Toxicity Analysis of 2-amino-1,3,4-thiadiazoles and Azo-1,3,4-thiadiazole Derivatives

The 2-amino-1,3,4-thiadiazole compounds **4a, 4b, 4d-e** showed higher viability percentage than the cytotoxicity against Peripheral Blood Lymphocyte (PBL) cells. The **4c** and **4h** compounds showed moderate viability percentage and higher toxicity. Moreover, all the azo-1,3,4-thiadiazole derivatives showed less toxicity and higher viability percentage against PBL cell lines.

4. SUMMARY AND CONCLUSION

- ✓ The 2-amino-1,3,4-thiadiazole derivatives were successfully synthesized with higher yield using a recyclable silica-supported catalyst.
- ✓ The structure of the compounds was confirmed with different spectroscopic techniques *viz* FTIR, NMR, Mass spectroscopy and elemental Analysis.
- ✓ FTIR, NMR spectroscopy analysis also confirmed the existence of azo-enol tautomerism of azo compounds.
- ✓ The compounds **4d** and **9d** showed the lowest HOMO-LUMO energy gap and highest dipole moment, responsible for their effective *in vitro* antibacterial activity.
- ✓ Energy calculations and NBO analysis revealed that the *trans* isomers are more stable than the *cis*-isomers.
- ✓ The compound **9d** effectively inhibited the *Staphylococcus aureus* at their 100 µg/mL concentration with 24 mm.
- ✓ The compound **4d** effectively inhibited biofilm formation against *Staphylococcus aureus* and *Pseudomonas aeruginosa*.

- ✓ The highest docking score was obtained for compound **9d**, consistent with the potent antibacterial activity.
- ✓ ADMET indicated good drug-likeness and pharmacokinetic nature of all the compounds.
- ✓ Overall, the results revealed that the 2-amino-1,3,4-thiadiazole with quinoline ring and quinoline-naphthol substituted azo derivatives showed potent inhibition activity. These scaffolds may serve as potent antibacterial in the future.

5. REFERENCES

- A. Santosh A. Jadhav *et al.*, Comparitive study of one pot synthetic methods of 2-amino-1,3,4-thiadiazole, *Der Pharma Chemica*, 2015, 7(2): 127-131.
- A. Valliammai, S. Sethupathy, A. Selvaraj, J.P. Bhaskar, V. Krishnan, S. K. Pandian. 2019, 9 (1). 13744. https://doi.org/10.1038/s41598-019-50207-y .
- Clinical Laboratory Standards Institute. Performance Standards for Antimicrobial Susceptibility Testing: Eighteenth Informational Supplement. CLSI Document M100-S18. Clinical Laboratory Standards Institute: Wayne, PA, USA, 2014.
- Discovery Studio for 3D Structures of docking Interactions- https://3ds.com/products-services/biovia/products?_gl=1*80ar15*_ga*NjYzNzcyODQzLjE2NDEzNDY2MTM.*_ga_DYJDKXYEZ4*MTY3MjU1MzA4My4xLjAuMTY3MjU1MzA4My42MC4wLjA.#_ga=2.171247529.826514732.1672553083-663772843.1641346613
- G. L. Almajan, S. F. Barbuceanu, G. Bancescu, I. Saramet, G. Saramet, C. Draghici, *Eur. J. Med. Chem*. 2010, 45, 6139 – 6146.
- K. Budziak, Makowski, Rachwał, Starzak, Matwijczuk, Myśliwa-Kurdziel, Oniszczuk, Combrzyński, Podleśna, Matwijczuk. *International Journal of Molecular Sciences* , (2019), *20(21), 5494–*. doi:10.3390/ijms20215494.
- K. Patil, R. Joshi-Navre, Mukherji and A. Prabhune. *Appl. Biochem. Biotechnol*. 2017, 181, 1533–1548. https://doi.org/10.1007/s12010-016-2300-8.
- K. Wiegand, K. Hilpert, R. Hancock. *Nature Protocols.* 2008, 3, 163–175. https://doi.org/10.1038/nprot.2007.521.
- L. Yijing, G. Jingkun Geng, L. Yang , Y. Shenghui, and Z. Guisen, *ChemMedChem* 2013, 8, 27 – 41.
- M. Hager, H.A. Ahmed, G. Aljohani, O. A. Alhaddad. *Int. J. Mol. Sci*. 2020, 21, 3922. http://dx.doi.org/10.3390/ijms21113922.
- M. Igarashi,T. Miyazawa The growth inhibitory effect of conjugated linoleic acid on a human hepatoma cell line, HepG2, is induced by a change in fatty acid metabolism, but not the facilitation of lipid peroxidation in the cells. Biochim Biophys Acta. 2001 Feb 26;1530(2-3):162-71.
- M. Ismael, A.M.M. Abdel-Mawgoud, M.K. Rabia, A. Abdou. *Inorg. Chim. Acta*. 2020, 505, 119443. https://doi.org/10.1016/j.ica.2020.119443.

- M. Kalia, V.K. Yadav, P.K. Singh, D. Sharma, H. Pandey, S.S. Narvi and V. Agarwal. *PLoS One*. 2015, 10. e0135495. https://doi.org/10.1371/journal.pone.0135495.
- M. Mahendrasinh . *et al.,* Synthesis and biological evaluation of some new 1,3,4-thiadiazole derivatives for their antimicrobial activities, *IJPCBS,* 2013, 3 (3):814-819.
- *M. Mahendrasinh et al.,* Synthesis, Characterization and antimicrobial evaluation of some 5-amino (substituted)-2-amino-thiodiazoles, *RJBCS,* 2013, 4 (3): 721 – 727.
- M. N. Noolvi, H. M. Patel, N. Singh, A. K. Gadad, S. S. Cameotra, A. Badiger, *Eur. J. Med. Chem*. 2011, 46, 4411 – 4418.
- M. Shamoradi, P. Faridifar, R. Shapouri, S. F. Mousavi, M.Ezzedin, B. Miraei. *Reports of Biochemistry & Molecular Biology*. 2019, 7. 181-188. http://rbmb.net/article-1-212-
- N.T. Rahmouni, B.N. Houda, S.A. Megatli, S. Djebbar, O.B. Baitich. *Spectrochim. Acta A Mol. Biomol. Spectrosc*. 2019, 213, 235−248. https://doi.org/10.1016/j.saa.2019.01.042.
- R. S. Lamani, N. S. Shetty, R. R. Kamble, I. A. Khazi, *Eur. J. Med. Chem*. 2009, 44, 2828 – 2833.
- R.B. Wallace, H.G. Jhon and M.U. George, phototropism and *cis-trans* isomerism in azo compounds, 1952.
- S. Ferrari, F. Morandi, D. Motiejunas, E, Nerjni, Stefan. Henrich, R. Luciani, A. Venturelli, S. Lazzari, Samuele. S. Gupta, V. Hannaert, P. A. M. Michels, R. C. Wade and M.P. Costi. *J. Med. Chem*. 2011, 54, 211–221. https://doi.org/10.1021/jm1010572
- S. S. Karki, K. Panjamurthy, S. Kumar, M. Nambiar, S. A. Ramareddy, K. K. Chiruvella, S. C. Raghavan, *Eur. J. Med. Chem*. 2011, 46, 2109 – 2116;
- SwissADME: a free web tool to evaluate pharmacokinetics, drug-likeness and medicinal chemistry friendliness of small molecules. *Sci. Rep.*2017; 7. 42717. .http://www.swissadme.ch/.
- T. Hatano, H. Kagawa, T. Yasuhara and T. Okuda, *Chem. Pharm. Bull*., 36, 6, 2090-2097 (1988) https://doi.org/10.1248/cpb.36.2090.
- T. Oleg, J.O. Arthur. Auto Dock Vina: Improving the speed and accuracy of docking with a new scoring function, efficient optimization, and multithreading. 2010, 30, 455-461. https://doi.org/10.1002/jcc.21334.
- Z. Lou, H. Wang, S. Rao, J. Sun, C. Ma, J. Li. *Food Control*. 2012, 25, 550-554. http://dx.doi.org/10.1016/j.foodcont.2011.11.022.